Electronic Supplementary Information

Sensing of peptide hormones with dynamic combinatorial libraries of metal-dye complexes: the advantage of time-resolved measurements

Friederike Zaubitzer, Thomas Riis-Johannessen and Kay Severin*

Institut des Sciences et Ingénierie Chimiques
École Polytechnique Fédérale de Lausanne (EPFL)
1015 Lausanne, Switzerland
Email: kay.severin@epfl.ch
Fax: +41(0)21 6939305; Tel: +41(0)21 6939302

Table S1 Molecular ions identified in the ESI mass spectra[a] during titrations of $MCl_2{\cdot}xH_2O$ ($M = Cu^{2+}$, $x = 2$; $M = Ni^{2+}$, $x = 6$) into aqueous solutions of Xylenol Orange ($[XO]_{tot}$ = 0.1 mM, pH 8.4).[b]

	M = Cu^{2+}		M = Ni^{2+}	
metal/dye ratio	*m/z*[c]	assignment	*m/z*[c]	assignment
0.5	335.24 (20)	$[XO+4H]^{2-}$	241.71 (100)	$[Ni(XO+H)]^{3-}$
	365.71 (30)	$[Cu(XO+2H)]^{2-}$	335.12 (30)	$[XO+4H]^{2-}$
			363.07 (60)	$[Ni(XO+2H)]^{2-}$
			391.03 (40)	$[Ni_2(XO)]^{2-}$
1.0	335.24 (20)	$[XO+4H]^{2-}$	391.03 (100)	$[Ni_2(XO)]^{2-}$
	365.71 (100)	$[Cu(XO+2H)]^{2-}$		
	396.18 (20)	$[Cu_2(XO)]^{2-}$		
1.5	396.18 (100)	$[Cu_2(XO)]^{2-}$	391.03 (100)	$[Ni_2(XO)]^{2-}$
2.0	396.18 (100)	$[Cu_2(XO)]^{2-}$	391.03 (100)	$[Ni_2(XO)]^{2-}$

[a] Negative mode. [b] We consider the dye as being fully ionised, i.e. all four carboxylic acid groups and two hydroxyl groups are deprotonated, such that XO ≡ $[XO]^{6-}$. [c] Relative intensity in parentheses.

Table S2 Molecular ions identified in the ESI mass spectra[a] during titrations of $MCl_2 \cdot xH_2O$ (M = Cu^{2+}, x = 2; M = Ni^{2+}, x = 6) into aqueous solutions of Arsenazo I ($[AI]_{tot}$ = 0.1 mM, pH 8.4).[b]

metal/dye ratio	M = Cu^{2+} *m/z*[c]	M = Cu^{2+} assignment	M = Ni^{2+} *m/z*[c]	M = Ni^{2+} assignment
0.5	201.96 (10)	$[Cu(AI+H)]^{3-}$	200.28 (5)	$[Ni(AI+H)]^{3-}$
	272.98 (100)	$[AI+4H]^{2-}$	272.98 (100)	$[AI+4H]^{2-}$
	303.45 (20)	$[Cu(AI+2H)]^{2-}$	300.91 (30)	$[Ni(AI+2H)]^{2-}$
1.0	201.96 (20)	$[Cu(AI+H)]^{3-}$	200.28 (5)	$[Ni(AI+H)]^{3-}$
	272.98 (100)	$[AI+4H]^{2-}$	272.98 (100)	$[AI+4H]^{2-}$
	303.45 (50)	$[Cu(AI+2H)]^{2-}$	300.91 (70)	$[Ni(AI+2H)]^{2-}$
1.5	201.96 (35)	$[Cu(AI+H)]^{3-}$	200.28 (10)	$[Ni(AI+H)]^{3-}$
	272.98 (100)	$[AI+4H]^{2-}$	272.98 (70)	$[AI+4H]^{2-}$
	303.45 (60)	$[Cu(AI+2H)]^{2-}$	300.91 (100)	$[Ni(AI+2H)]^{2-}$
2.0	201.96 (35)	$[Cu(AI+H)]^{3-}$	200.28 (10)	$[Ni(AI+H)]^{3-}$
	272.98 (100)	$[AI+4H]^{2-}$	272.98 (50)	$[AI+4H]^{2-}$
	303.45 (95)	$[Cu(AI+2H)]^{2-}$	300.91 (100)	$[Ni(AI+2H)]^{2-}$

[a] Negative mode. [b] We consider the dye as being fully ionised, i.e. the sulphonate, arsenate and hydroxyl functionalities are all fully deprotonated, such that AI ≡ $[AI]^{6-}$. [c] Relative intensity in parentheses.

Table S3 Molecular ions identified in the ESI mass spectra[a] during titrations of $MCl_2 \cdot xH_2O$ ($M = Cu^{2+}$, $x = 2$; $M = Ni^{2+}$, $x = 6$) into aqueous solutions of Methyl Calcein Blue ($[MCB]_{tot}$ = 0.1 mM, pH 8.4).[b]

	M = Cu^{2+}		M = Ni^{2+}	
metal/dye ratio	*m/z*[c]	assignment	*m/z*[c]	assignment
0.5	276.24 (100)	$[MCB+H]^-$	276.24 (100)	$[MCB+H]^-$
	373.19 (5)	$[Cu(MCB+H)(OH)_2]^-$		
1.0	276.24 (40)	$[MCB+H]^-$	368.19 (100)	$[Ni(MCB+H)(OH)_2]^-$
	373.19 (100)	$[Cu(MCB+H)(OH)_2]^-$		
1.5	276.24 (10)	$[MCB+H]^-$	368.19 (100)	$[Ni(MCB+H)(OH)_2]^-$
	373.19 (100)	$[Cu(MCB+H)(OH)_2]^-$		
2.0	276.24 (10)	$[MCB+H]^-$	368.19 (100)	$[Ni(MCB+H)(OH)_2]^-$
	373.19 (100)	$[Cu(MCB+H)(OH)_2]^-$		

[a] Negative mode. [b] We consider the dye as being fully ionised, i.e. both carboxylic acid and hydroxyl functionalities are all fully deprotonated, such that MCB ≡ $[MCB]^{2-}$. [c] Relative intensity in parentheses.

Table S4 Molecular ions identified in the ESI mass spectra[a] during titrations of $MCl_2 \cdot xH_2O$ ($M = Cu^{2+}$, $x = 2$; $M = Ni^{2+}$, $x = 6$) into aqueous solutions of Methyl Calcein Blue ($[MCB]_{tot}$ = 50 μM, pH 8.4), Arsenazo I ($[AI]_{tot}$ = 25 μM, pH 8.4) and Xylenol Orange ($[XO]_{tot}$ = 12.5 μM, pH 8.4), .[b]

$M = Cu^{2+}$, $M = Ni^{2+}$	
m/z[c]	assignment
272.96 (100)	$[AI+4H]^{2-}$
303.42 (60)	$[Cu(AI+2H)]^{2-}$
300.92 (40)	$[Ni(AI+2H)]^{2-}$
441.96 (10)	$[Cu(AI+MCB+4H)]^{2-}$
439.46 (10)	$[Ni(AI+MCB+4H)]^{2-}$
396.00 (20)	$[Cu_2(XO)]^{2-}$
393.50 (20)	$[CuNi(XO)]^{2-}$
390.99 (20)	$[Ni_2(XO)]^{2-}$

[a] Negative mode. [b] We consider all dyes as being fully ionised, i.e. all carboxylic acid, sulfonate, arsenate and hydroxyl groups are deprotonated. [c] Relative intensity in parentheses.

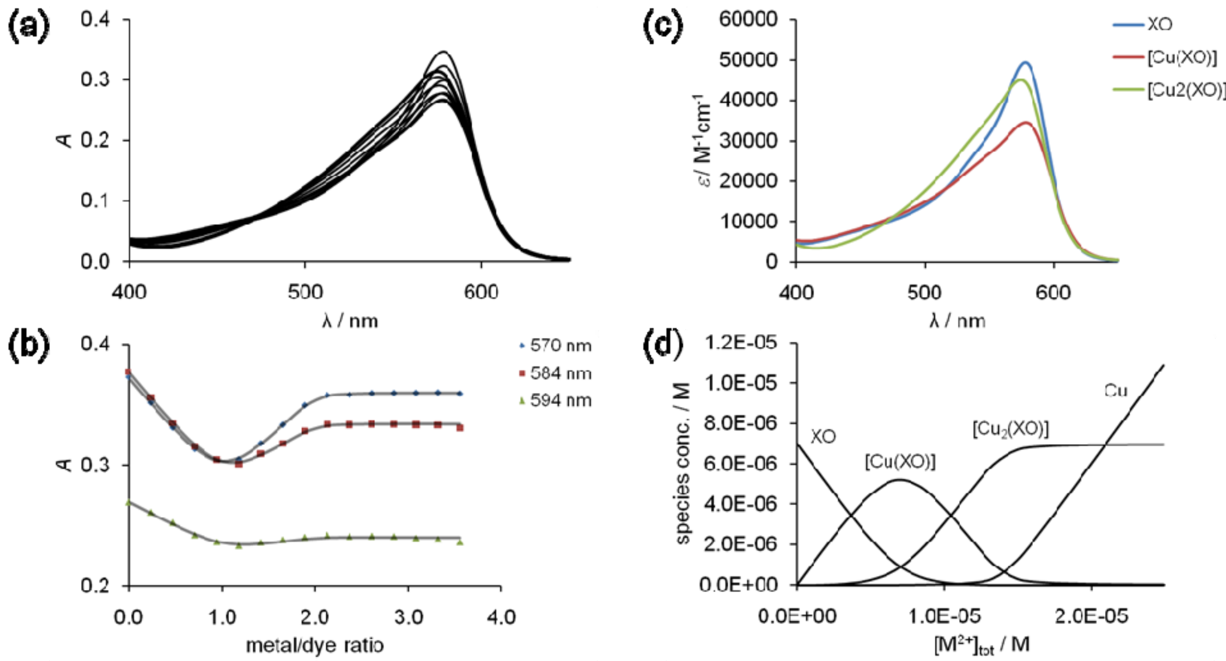

Fig. S1 (a) Observed changes in the UV-Vis spectrum of a buffered aqueous solution of Xylenol Orange ($[XO]_{tot}$ = 7.5 μM, CHES buffer, 0.1 M, pH 8.4, 298 K) upon addition of $CuCl_2{\cdot}2H_2O$ ($[Cu^{2+}]_{aq}$ = 5 mM). (b) Variation in absorbance vs. metal/ligand ratio for three selected wavelengths (the line represents the best fit to the models discussed in the main text). (c) Calculated absorption spectra of the three coloured species included in the model. (d) Calculated species distribution diagram for the metal, dye and the two complexes as a function of total metal concentration.

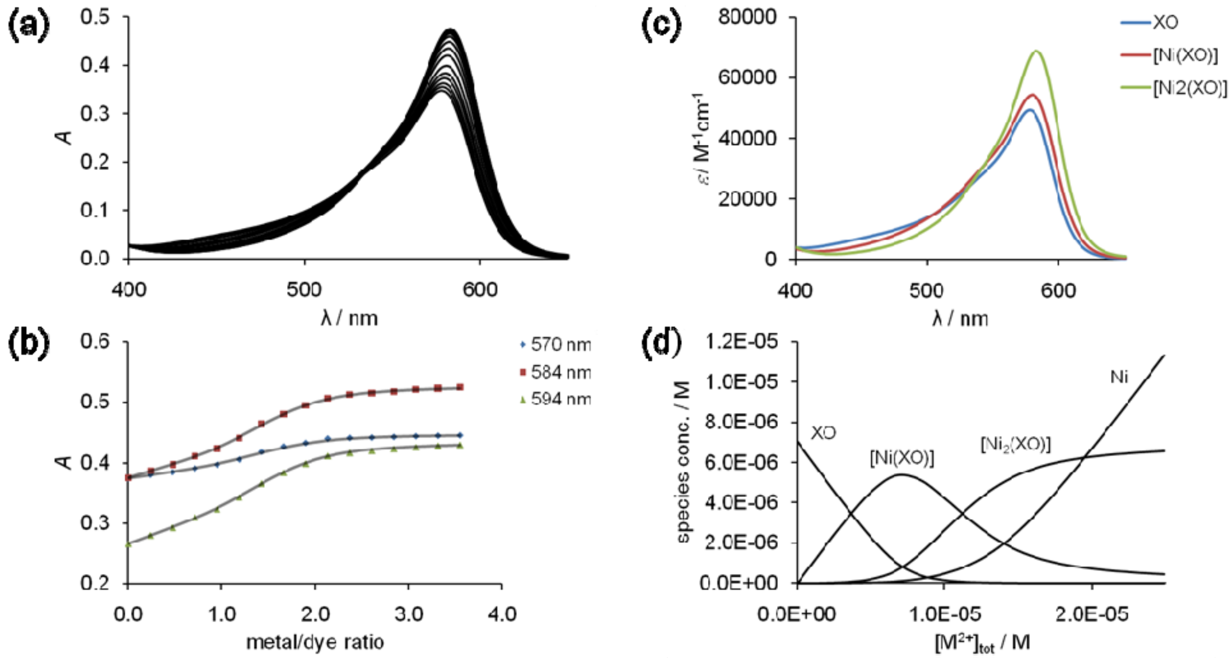

Fig. S2 (a) Observed changes in the UV-Vis spectrum of a buffered aqueous solution of Xylenol Orange ($[XO]_{tot}$ = 7.5 μM, CHES buffer, 0.1 M, pH 8.4, 298 K) upon addition of $NiCl_2 \cdot 6H_2O$ ($[Ni^{2+}]_{aq}$ = 5 mM). (b) Variation in absorbance vs. metal/ligand ratio for three selected wavelengths (the line represents the best fit to the models discussed in the main text). (c) Calculated absorption spectra of the three coloured species included in the model. (d) Calculated species distribution diagram for the metal, dye and the two complexes as a function of total metal concentration.

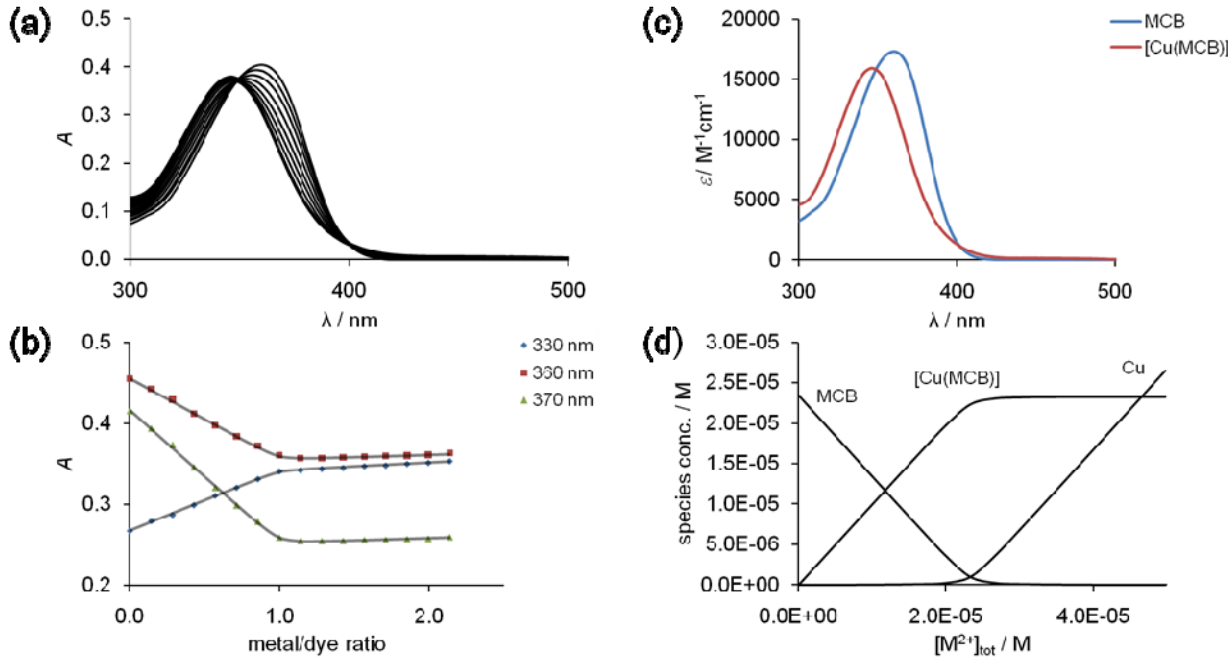

Fig. S3 (a) Observed changes in the UV-Vis spectrum of a buffered aqueous solution of Methyl Calcein Blue ($[MCB]_{tot}$ = 25 μM, CHES buffer, 0.1 M, pH 8.4, 298 K) upon addition of $CuCl_2{\cdot}2H_2O$ ($[Cu^{2+}]_{aq}$ = 10 mM). (b) Variation in absorbance vs. metal/ligand ratio for three selected wavelengths (the line represents the best fit to the models discussed in the main text). (c) Calculated absorption spectra of the two coloured species included in the model. (d) Calculated species distribution diagram for the metal, dye and complex as a function of total metal concentration.

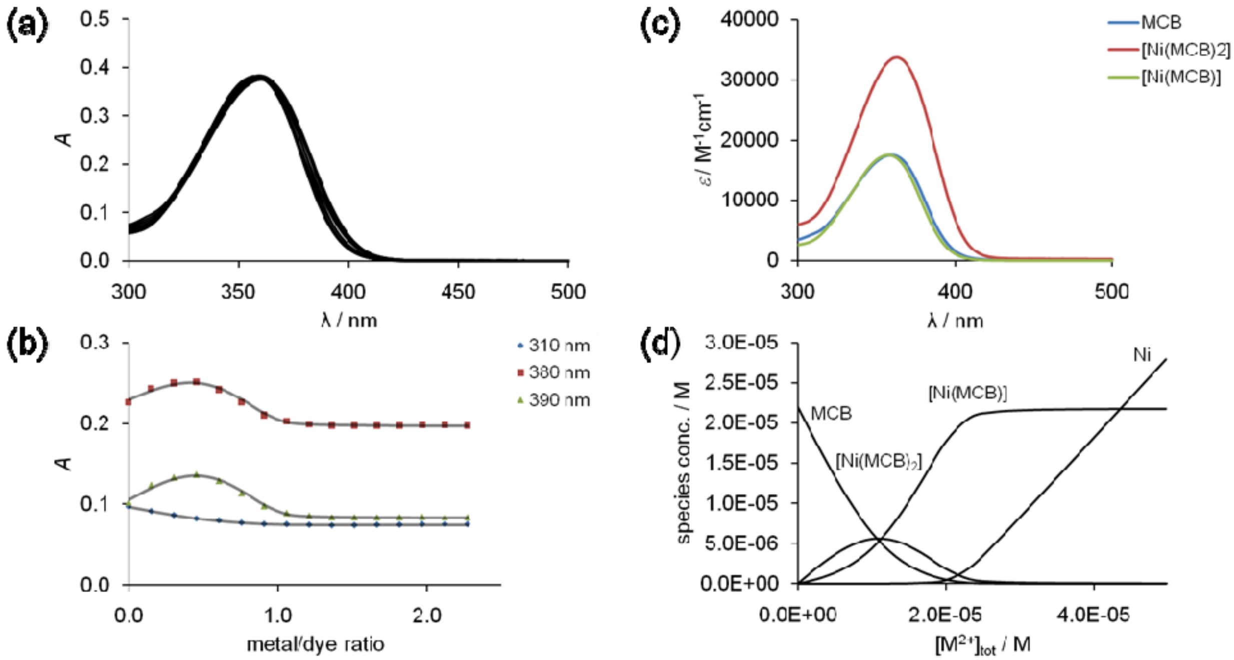

Fig. S4 (a) Observed changes in the UV-Vis spectrum of a buffered aqueous solution of Methyl Calcein Blue ($[MCB]_{tot}$ = 25 μM, CHES buffer, 0.1 M, pH 8.4, 298 K) upon addition of $NiCl_2 \cdot 6H_2O$ ($[Ni^{2+}]_{aq}$ = 10 mM). (b) Variation in absorbance vs. metal/ligand ratio for three selected wavelengths (the line represents the best fit to the models discussed in the main text). (c) Calculated absorption spectra of the three coloured species included in the model. (d) Calculated species distribution diagram for the metal, dye and the two complexes as a function of total metal concentration.

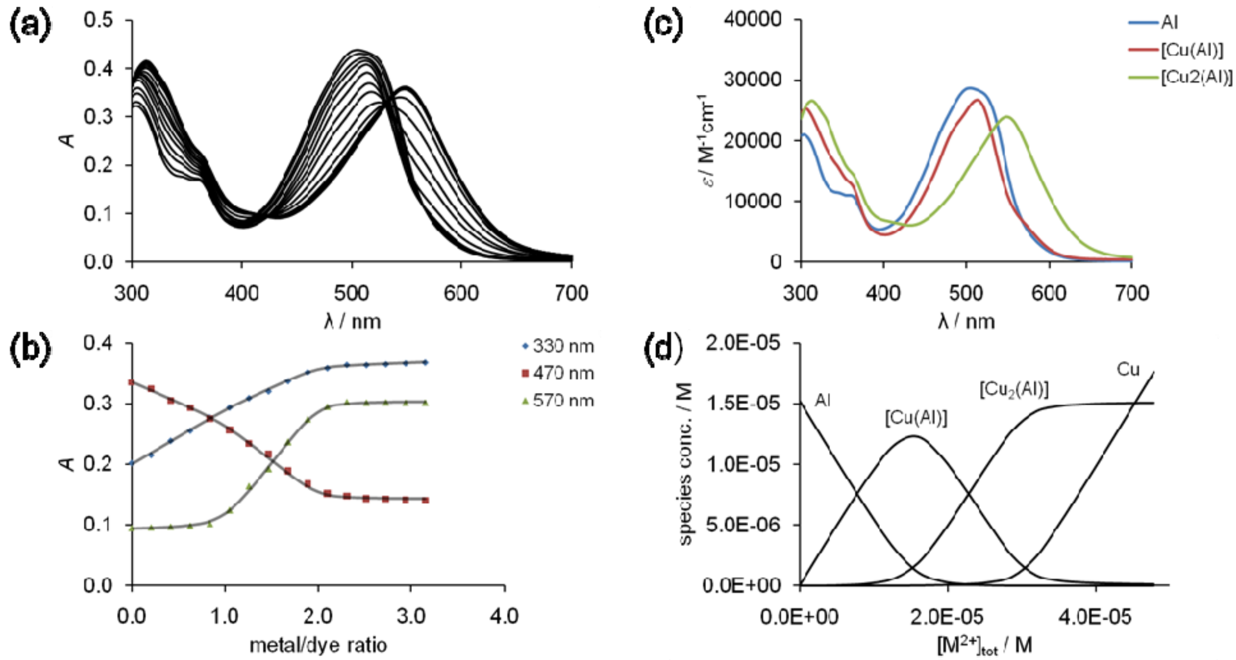

Fig. S5 (a) Observed changes in the UV-Vis spectrum of a buffered aqueous solution of Arsenazo I ($[AI]_{tot}$ = 15 µM, CHES buffer, 0.1 M, pH 8.4, 298 K) upon addition of $CuCl_2{\cdot}2H_2O$ ($[Cu^{2+}]_{aq}$ = 10 mM). (b) Variation in absorbance vs. metal/ligand ratio for three selected wavelengths (the line represents the best fit to the models discussed in the main text). (c) Calculated absorption spectra of the three coloured species included in the model. (d) Calculated species distribution diagram for the metal, dye and the two complexes as a function of total metal concentration.

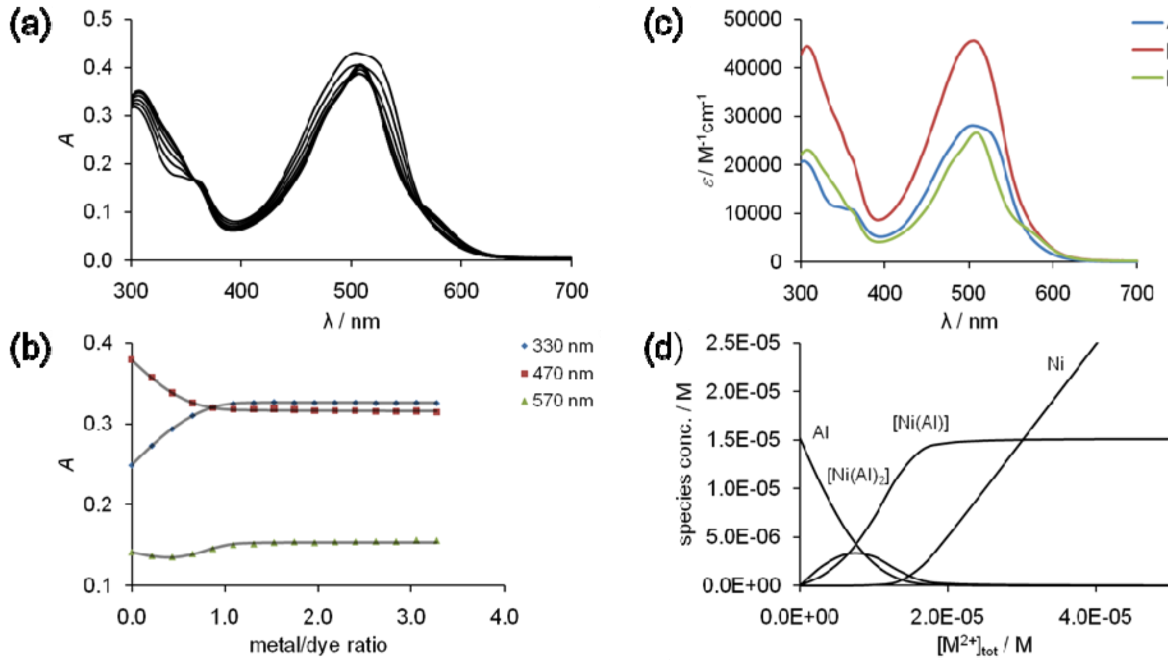

Fig. S6 (a) Observed changes in the UV-Vis spectrum of a buffered aqueous solution of Arsenazo I ($[AI]_{tot}$ = 15 µM, CHES buffer, 0.1 M, pH 8.4, 298 K) upon addition of $NiCl_2{\cdot}6H_2O$ ($[Ni^{2+}]_{aq}$ = 10 mM). (b) Variation in absorbance vs. metal/ligand ratio for three selected wavelengths (the line represents the best fit to the models discussed in the main text). (c) Calculated absorption spectra of the three coloured species included in the model. (d) Calculated species distribution diagram for the metal, dye and the two complexes as a function of total metal concentration.

Linear Discriminant Analyses

a) DCL sensor read-out at *t* = 24h:

Classification matrix (cases in row categories classified into columns):

	0.1AngI/ 0.9AngII	0.2AngI/ 0.8AngII	0.3AngI/ 0.7AngII	0.4AngI/ 0.6AngII	0.5AngI/ 0.5AngII	0.6AngI/ 0.4AngII
0.1AngI/0.9AngII	4	1	0	0	0	0
0.2AngI/0.8AngII	1	2	0	2	1	0
0.3AngI/0.7AngII	0	0	5	1	0	0
0.4AngI/0.6AngII	0	1	0	4	1	0
0.5AngI/0.5AngII	0	0	0	0	6	0
0.6AngI/0.4AngII	0	0	0	0	0	6
0.7AngI/0.3AngII	0	0	0	0	0	0
0.8AngI/0.2AngII	0	0	0	0	0	0
0.9AngI/0.1AngII	0	0	0	0	0	0
AngI	0	0	0	0	0	0
AngII	0	0	0	0	0	0
total	5	4	5	7	8	6

	0.7AngI/ 0.3AngII	0.8AngI/ 0.2AngII	0.9AngI/ 0.1AngII	AngI	AngII	%correct
0.1AngI/0.9AngII	0	0	0	0	1	67
0.2AngI/0.8AngII	0	0	0	0	0	33
0.3AngI/0.7AngII	0	0	0	0	0	83
0.4AngI/0.6AngII	0	0	0	0	0	67
0.5AngI/0.5AngII	0	0	0	0	0	100
0.6AngI/0.4AngII	0	0	0	0	0	100
0.7AngI/0.3AngII	6	0	0	0	0	100
0.8AngI/0.2AngII	0	4	2	0	0	67
0.9AngI/0.1AngII	0	0	6	0	0	100
AngI	0	0	0	6	0	100
AngII	0	0	0	0	6	100
total	6	4	8	6	7	**83**

Jackknifed classification matrix (Each measurement used for the training set was omitted once and then classified.):

	0.1AngI/ 0.9AngII	0.2AngI/ 0.8AngII	0.3AngI/ 0.7AngII	0.4AngI/ 0.6AngII	0.5AngI/ 0.5AngII	0.6AngI/ 0.4AngII
0.1AngI/0.9AngII	4	1	0	0	0	0
0.2AngI/0.8AngII	2	1	0	2	1	0
0.3AngI/0.7AngII	0	0	5	1	0	0
0.4AngI/0.6AngII	0	2	0	3	1	0
0.5AngI/0.5AngII	0	0	0	0	6	0
0.6AngI/0.4AngII	0	0	0	0	0	6
0.7AngI/0.3AngII	0	0	0	0	0	1
0.8AngI/0.2AngII	0	0	0	0	0	0
0.9AngI/0.1AngII	0	0	0	0	0	0
AngI	0	0	0	0	0	0
AngII	2	1	0	0	0	0
total	8	5	5	6	8	7

	0.7AngI/ 0.3AngII	0.8AngI/ 0.2AngII	0.9AngI/ 0.1AngII	AngI	AngII	%correct
0.1AngI/0.9AngII	0	0	0	0	1	67
0.2AngI/0.8AngII	0	0	0	0	0	17
0.3AngI/0.7AngII	0	0	0	0	0	83
0.4AngI/0.6AngII	0	0	0	0	0	50
0.5AngI/0.5AngII	0	0	0	0	0	100
0.6AngI/0.4AngII	0	0	0	0	0	100
0.7AngI/0.3AngII	4	1	0	0	0	67
0.8AngI/0.2AngII	1	3	2	0	0	50
0.9AngI/0.1AngII	0	1	5	0	0	83
AngI	0	0	0	6	0	100
AngII	0	0	0	0	3	50
total	5	5	7	6	4	**70**

Eigenvalues:

40.371	1.440	0.595	0.158

Canonical correlations:

0.988	0.768	0.611	0.370

Cumulative proportion of total dispersion:

0.948	0.982	0.996	1.000

b) Time-resolved analysis of the DCL sensor:

Classification matrix (cases in row categories classified into columns):

	0.1AngI/ 0.9AngII	0.2AngI/ 0.8AngII	0.3AngI/ 0.7AngII	0.4AngI/ 0.6AngII	0.5AngI/ 0.5AngII	0.6AngI/ 0.4AngII
0.1AngI/0.9AngII	6	0	0	0	0	0
0.2AngI/0.8AngII	0	6	0	0	0	0
0.3AngI/0.7AngII	0	0	6	0	0	0
0.4AngI/0.6AngII	0	0	0	6	0	0
0.5AngI/0.5AngII	0	0	0	0	6	0
0.6AngI/0.4AngII	0	0	0	0	0	6
0.7AngI/0.3AngII	0	0	0	0	0	0
0.8AngI/0.2AngII	0	0	0	0	0	0
0.9AngI/0.1AngII	0	0	0	0	0	0
AngI	0	0	0	0	0	0
AngII	0	0	0	0	0	0
total	6	6	6	6	6	6

	0.7AngI/ 0.3AngII	0.8AngI/ 0.2AngII	0.9AngI/ 0.1AngII	AngI	AngII	%correct
0.1AngI/0.9AngII	0	0	0	0	0	100
0.2AngI/0.8AngII	0	0	0	0	0	100
0.3AngI/0.7AngII	0	0	0	0	0	100
0.4AngI/0.6AngII	0	0	0	0	0	100
0.5AngI/0.5AngII	0	0	0	0	0	100
0.6AngI/0.4AngII	0	0	0	0	0	100
0.7AngI/0.3AngII	6	0	0	0	0	100
0.8AngI/0.2AngII	0	6	0	0	0	100
0.9AngI/0.1AngII	0	0	6	0	0	100
AngI	0	0	0	6	0	100
AngII	0	0	0	0	6	100
total	6	6	6	6	6	**100**

Jackknifed classification matrix (Each measurement used for the training set was omitted once and then classified.):

	0.1AngI/ 0.9AngII	0.2AngI/ 0.8AngII	0.3AngI/ 0.7AngII	0.4AngI/ 0.6AngII	0.5AngI/ 0.5AngII	0.6AngI/ 0.4AngII
0.1AngI/0.9AngII	4	0	0	0	0	0
0.2AngI/0.8AngII	0	4	1	0	1	0
0.3AngI/0.7AngII	0	1	4	0	1	0
0.4AngI/0.6AngII	0	0	0	5	1	0
0.5AngI/0.5AngII	0	0	0	0	6	0
0.6AngI/0.4AngII	0	0	0	0	0	6
0.7AngI/0.3AngII	0	0	0	0	0	0
0.8AngI/0.2AngII	0	0	0	0	0	0
0.9AngI/0.1AngII	0	0	0	0	0	0
AngI	0	0	0	0	0	0
AngII	3	0	0	0	0	0
total	7	5	5	5	9	6

	0.7AngI/ 0.3AngII	0.8AngI/ 0.2AngII	0.9AngI/ 0.1AngII	AngI	AngII	%correct
0.1AngI/0.9AngII	0	0	0	0	2	67
0.2AngI/0.8AngII	0	0	0	0	0	67
0.3AngI/0.7AngII	0	0	0	0	0	67
0.4AngI/0.6AngII	0	0	0	0	0	83
0.5AngI/0.5AngII	0	0	0	0	0	100
0.6AngI/0.4AngII	0	0	0	0	0	100
0.7AngI/0.3AngII	5	1	0	0	0	83
0.8AngI/0.2AngII	0	6	0	0	0	100
0.9AngI/0.1AngII	0	1	5	0	0	83
AngI	0	0	0	6	0	100
AngII	0	0	0	0	3	50
total	5	8	5	6	5	**82**

Eigenvalues:

131.171	3.670	2.101	1.189	0.923	0.597	0.366	…

Canonical correlations:

0.996	0.886	0.823	0.737	0.693	0.612	0.518	…

Cumulative proportion of total dispersion:

0.935	0.961	0.976	0.984	0.991	0.995	0.998	…